Received: 8 April 2022 | Revised: 29 June 2022 | Accepted: 22 August 2022

DOI: 10.1002/qua.27019

RESEARCH ARTICLE

International Journal of Quantum Chemistry WILEY

Aufbau principle and singlet-triplet gap in spherical Hooke atoms

Xabier Telleria-Allika[1] | Jesus M. Ugalde[1] | Eduard Matito[2,3] | Eloy Ramos-Cordoba[2,3] | Mauricio Rodríguez-Mayorga[4] | Xabier Lopez[1]

[1]Polimero eta Material Aurreratuak: Fisika, Kimika eta Teknologia, Kimika Fakultatea, Euskal Herriko Unibertsitatea UPV/EHU, Donostia, Spain

[2]Donostia International Physics Centre (DIPC), Donostia, Spain

[3]IKERBASQUE, Basque Foundation for Science, Bilbao, Spain

[4]DEN, Service de Recherches de Métallurgie Physique, CEA, Université Paris-Saclay, Gif-sur-Yvette, France

Correspondence
Xabier Lopez, Polimero eta Material Aurreratuak: Fisika, Kimika eta Teknologia, Kimika Fakultatea, Euskal Herriko Unibertsitatea UPV/EHU, PK 1072, 20080 Donostia, Euskadi, Spain.
Email: xabier.lopez@ehu.eus

Funding information
Eusko Jaurlaritza, Grant/Award Numbers: IT1254-19, IT1584-22, PIBA19-0004, 2019-CIEN-000092-01; Juan de la Cierva program, Grant/Award Number: IJCI-2017-34658; Spanish MINECO/FEDER, Grant/Award Numbers: EUR2019-103825, EUIN2017-88605, PGC2018-098212-B-C21, PGC2018-097529-B-100

Abstract

Singlet and triplet spin state energies for three-dimensional Hooke atoms, that is, electrons in a quadratic confinement, with even number of electrons (2, 4, 6, 8, 10) is discussed using Full-CI and CASSCF type wavefunctions with a variety of basis sets and considering perturbative corrections up to second order. The effect of the screening of the electron–electron interaction is also discussed by using a Yukawa-type potential with different values of the Yukawa screening parameter ($\lambda_{ee} = 0.2$, 0.4, 0.6, 0.8, 1.0). Our results show that the singlet state is the ground state for two and eight electron Hooke atoms, whereas the triplet is the ground spin state for 4-, 6-, and 10-electron systems. This suggests the following Aufbau structure $1s < 1p < 1d$ with singlet ground spin states for systems in which the generation of the triplet implies an inter-shell one-electron promotion, and triplet ground states in cases when there is a partial filling of electrons of a given shell. It is also observed that the screening of electron–electron interactions has a sizable quantitative effect on the relative energies of both spin states, specially in the case of two- and eight-electron systems, favoring the singlet state over the triplet. However, the screening of the electron–electron interaction does not provoke a change in the nature of the ground spin state of these systems. By analyzing the different components of the energy, we have gained a deeper understanding of the effects of the kinetic, confinement and electron–electron interaction components of the energy.

KEYWORDS
electron correlation, Hooke atoms, optimized Gaussian basis functions, Yukawa screening potential

1 | INTRODUCTION

Quantum dots have attracted considerable attention in the last years. The possibility of creating artificial atoms in which the electrons are confined to a center through a quadratic type potential opens the possibility of designing new nanoelectronic devices with properties at will, by precisely controlling the degree of confinement. For instance, transitions never observed in natural atoms can be obtained in the artificial ones, which could be of paramount importance in designing new lasers [1]. Another property that has attracted considerable attention is the

determination of the triplet-singlet gap in confined systems, for their use as states of a qubit, or to implement logical gates in quantum computing [2, 3]. The excitation spectrum of two-electron two-dimensional (2D) quantum dots has been investigated by tunneling spectroscopy [4], and the theoretical prediction of triplet-singlet transitions with increasing magnetic field has been experimentally corroborated. Although less studied, 3D quantum dots are also a subject of interest [5]. Examples of this are magnetically trapped fermion vapors confined by parabolic potentials [6, 7] or quantum defects in diamond crystals used as basic gadgets in quantum computing [8, 9].

One of the simplest and most adequate models used in theoretical studies concerning QDs are the so-called Harmonium or Hooke's atom in which electrons are confined in a spherical harmonic potential [10]. Such models contain parameters that may be tuned in order to represent features corresponding to real QDs [11, 12]. For instance, work carried out in our group using a Hookean exact three-body model to examine electron correlation in a two-electron spherical quantum dot confirmed that triplet-singlet transitions take place as the externally applied magnetic field increases [13]. However, the limitation of using an exact model restricted our study to two-electron systems. That is, the analytical solutions [14] for the curvature parameter of the two-electron Hooke atoms ($\omega^2 = 1/4, 1/100, \ldots$) are well known, which can lead in principle to highly accurate densities for systems in low-correlation regimes ($\omega^2 \to \infty$) as well as in high-correlation regimes ($\omega^2 \to 0$) [15–18]. If similar systems containing larger number of electrons ($N > 2$) are to be considered, a richer variety of electronic states consisting of several ground state spin multiplicities and nondynamical electron correlation (multi-determinantal features) arise [19–21]. Although such systems can be employed to understand many-body interactions, the computational cost increases with the size of the system.

As in Hooke model atoms, the incorporation of electron correlation effects has been shown to be essential for an adequate interpretation of the experimental spectra and transport properties in Quantum Dots [5, 22–25]. In quantum dots, as opposed to real atoms, the effect of electron correlation may be varied at will through manipulation of the dimension and shape of the nanocrystal as well as of the strength, boundaries, and symmetries of the confining fields [26]. Besides, the electron–electron interaction can be screened due to lattice, the doping or the charges induced on the metal gates [27]. This fact makes the quantum dot many-body problem more complex than the more familiar atomic case.

Finally, Hooke model systems have been repeatedly used in the calibration of electronic structure methods, for they provide very variable dynamic and non-dynamic electron correlation regimes. Finally, Hooke model systems have been repeatedly used in the calibration of electronic structure methods, for they provide very variable dynamic and non-dynamic electron correlation regimes [28–30] that pose a great challenge for current computational methods [17, 31–43]. Such calibration has been possible because of the recent availability of highly accurate analytical and benchmark data [19, 20, 28–30, 44–50] that pose a great challenge for current computational methods [17, 31–43].

Several well established methods for the elucidation of atomic/molecular electronic structure have been applied to quantum dots. Salient among these are diagonalizations of large configuration interaction representations of the Hamiltonian matrix (usually referred as "exact" diagonalizations) [51–56], Hartree–Fock (HF) [54, 57–59], coupled-cluster [60], density functional theory [61–64], and quantum Monte Carlo calculations [65]. Let us emphasize, however, that even for two-electron quantum dots [66], it has been observed that in order to account properly for the electron correlation effects, one must go beyond perturbative schemes based on the independent-particle model or local spin-density functional theory [4]. Last but not least, some of us have found that the use of flexible basis set is crucial for a correct description of strong correlation effects in harmonium [20, 40, 66].

In the present paper, we address the orbital occupation pattern to establish the Aufbau principle for three-dimensional quantum dots with an even number of electrons ($N = 2, 4, 6, 8, 10$). Full configuration interaction (Full-CI) for $N = 2$, and complete active space self-consistent field (CASSCF) type wavefunctions, for $N > 2$, are employed to account for electron correlation effects. On top of this, second-order perturbation corrections to these energies are also considered. Both the singlet and the triplet states will be evaluated in order to ascertain whether the ground state wavefunction is either spin unpolarized or spin polarized. This will provide, by the same token, the estimate of the triplet-singlet energy gap as the number of electrons of the quantum dots increases.

First, we have employed the Dunning's family of correlation consistent (CC) basis sets up to sextuple zeta. One should notice that these basis sets are optimized for Coulombic systems, and, therefore, for the sake of consistency, we have compared their accuracy with the available benchmark data [19, 21, 48, 66]. We report the full data as Data S1. In summary, although these absolute energies do not reach full accuracy, the singlet-triplet gaps were in full agreement with the benchmark data, except for the 10-electron system for which qualitative differences were observed depending on which CC basis set was used. In order to further improve the performance of the basis set, we have optimized a set of even-tempered basis sets (ETBS hereafter) for the Hooke potential considering different number of electrons. After careful inspection, the best balance between accuracy and performance was obtained for the basis set optimized with six electrons in the singlet state, we call this basis set ETBS-6S, and it is the one mainly used throughout the paper.

2 | COMPUTATIONAL METHODS

Let us consider the following generalized Hamiltonian operator (in atomic units) for our N-electron system:

$$\hat{H} = -\frac{1}{2}\sum_i^N \nabla_{r_i}^2 + \frac{1}{2}\omega^2 \sum_i^N r_i^2 + \sum_i^N \sum_{j>i}^N \frac{e^{-\lambda_{ee} r_{ij}}}{r_{ij}} \quad (1)$$

where $\mathbf{r}_i$ is the distance vector between the ith electron and the center of the harmonic potential, which for all the calculations of this paper is centered at the origin. This Hamiltonian represents a harmonically confined N-electron system, with a confinement strength ω^2, whose inter-electronic interaction has been screened staticall by a Yukawa-like attenuated interaction potential, having a screening length λ^{-1}.

Recall that for $N = 2$ and $\lambda_{ee} = 0$, the Hamiltonian operator of Equation (1) corresponds to the two-electron Hooke atom, which can be separated into its intracular coordinates, namely, the electron–electron relative distance vector $\mathbf{r} = \mathbf{r}_1 - \mathbf{r}_2$ and the center of mass coordinate vector $\mathbf{R} = ½ (\mathbf{r}_1 + \mathbf{r}_2)$ as [14, 67]

$$\widehat{H} = -\frac{\nabla_R^2}{4} + \omega^2 R^2 - \nabla_r^2 + \frac{1}{4}\omega^2 r^2 + \frac{1}{r} \tag{2}$$

being $r = |\mathbf{r}|$ and $\boldsymbol{R} = |\mathbf{R}|$, respectively. Equation (2) unveils that the center of mass of the electrons will behave as a harmonic oscillator with a spring constant of $2\omega^2$ and a ground state energy of $\boldsymbol{E}_{\mathbf{R}} = 3\ \omega$. Likewise, Equation (2) indicates as well, that the electrons will remain in the proximity of each other for they are retained by the potential

$$V(r) = \frac{1}{4}\omega^2 r^2 + \frac{1}{r} \tag{3}$$

which is best seen as an effective confinement potential. This model system is commonly known as Hooke atom, Hookean, or harmonium [68]. In summary, two types of systems have been considered in this paper:

1. *Coulombic Hooke Atom*: The Hamiltonian includes an harmonic confinement term ($\omega^2 = 0.25$) with Coulombic like electron–electron repulsion ($\lambda_{ee} = 0.0$).
2. *Yukawa Hooke Atom*: The Hamiltonian includes an harmonic confinement term ($\omega^2 = 0.25$) and a Yukawa-type screened electron repulsion ($\lambda_{ee} = 0.2, 0.4, 0.6, 0.8,$ and 1.0).

The corresponding one-electron confinement integrals and the two-electron Yukawa-type integrals have been implemented by our group in an in-house code and the corresponding integral package interfaced with the GAMESS(US) program [69, 70] to perform the calculations described in this work. HF, Full-CI, CASSCF and multireference second-order Möller–Plesset (MRMP2) methods were used along with various basis sets of aug-cc type, and optimized ETBS for 2, 4, 6, and 8 electrons systems. For each of the systems, the HF energy of the singlet state was calculated. The corresponding orbitals were used to perform Full-CI (in the case of two-electron systems) and CASSCF and MRMP2 calculations (in the case of 2, 4, 6, 8, and 10 electrons) for the singlet and triplet spin states.

As said in the introduction, we have employed two types of basis sets: (i) standard Dunning's family of correlation consistent (cc) basis sets up to sextuple zeta and (ii) ETBS optimized for the Hooke atom. The drawback of aug-cc-pV*N*Z basis sets is that they are optimized for Coulombic systems. Therefore, we have compared their accuracy with the available benchmark data [19, 21, 48, 66] for Hookean systems. We report the full data as Data S1, but in summary, the conclusion is that, although absolute energies with aug-cc-pV*N*Z basis sets do not reach full accuracy, the singlet-triplet gaps are in full agreement with the benchmark data. The only exception to this rule is the 10-electron system, which shows a more erratic behavior with important qualitative differences concerning the ground state spin multiplicity among the various aug-cc-pV*N*Z basis sets.

In order to improve the absolute energies, we have optimized an ETBS in the presence of a harmonic potential ($\omega^2 = 0.25$) considering different numbers of electrons. We have employed uncontracted ETBS with angular momentum $L = 0$ to $L = 3$ and the same number N of primitives per shell. The L and N dependent exponents of the primitives are even-tempered following the scheme:

$$\zeta_{LN}^k(\omega^2) = \frac{\omega^2}{2}\alpha_{LN}(\omega^2)\left[\beta_{LN}(\omega^2)\right]^{k-1}, 1 \le k \le N \tag{4}$$

where the parameters α and β are optimized by minimizing the CASSCF (full electron and 13 active orbitals) energies. Similar strategies have been followed in previous publications [42, 66, 71].

After careful inspection, the best balance between accuracy and performance was obtained for the basis set optimized with six electrons in the singlet state, we call this basis set the ETBS-6S. This basis set can be characterized as an uncontracted 4(SPDF) basis set for which the parameters given in the Equation (4) are $\alpha_{L,N} = 1.923456$ and $\beta_{L,N} = 1.3021162$ which give rise to the following exponent values: 0.2404032, 0.3130329, 0.4076051, 0.5307491. The total number of basis sets is 80, out of which 68 are linearly independent and these are the only one used in the calculations. The results for this basis set showed a better agreement in both absolute energies and singlet-triplet gaps with respect to the available benchmark data than the standard aug-cc-pV*N*Z series, and therefore, we focus our discussion on the results obtained with this basis set.

3 | RESULTS AND DISCUSSION

This section is organized in accordance to the number of electrons of the system. Thus, we start our discussion with two-electron systems, and then 4-, 6-, 8-, and 10-electron systems follow. In the case of the two-electron Coulombic Hooke atom, the exact energy is known [14, 67], and therefore, there is a benchmark value to calibrate the basis sets employed throughout this work. In the other cases, we will use the benchmark data available in the literature [19, 21, 48, 66]. Thus, the first section is dedicated to this calibration. Then, the discussion is centered on the triplet-singlet gap for each of the systems, focusing our discussion on the factors that affect this gap, such as the electron repulsion screening and the number of electrons in the system. To understand these trends, we analyze the corresponding natural orbitals, so that we can relate the solution to a specific electronic configuration. Based on this information, we come up with an *Aufbau* structure to describe the electron filling pattern in these confined systems.

3.1 | Two-electron systems

The results for the two-electron Hooke-type atom with Coulombic electron repulsion are shown in Table 1. We emphasize that for this system the exact energy for the singlet state is known [14, 67], namely 2.0 a.u., and, therefore, we use this reference value to calibrate the accuracy of the various basis sets used throughout this work (Table 1). There is a substantial difference between aug-cc-pVDZ and the rest of the basis sets. Full-CI energy for the singlet state is 2.055213 a.u. with this basis set. The use of aug-cc-pVTZ (25 basis functions including d orbitals) leads to a reduction of the energy error of one order of magnitude, leading to a Full-CI energy of 2.004107 a.u. To further reduce the energy error by one order of magnitude, one has to go up to the aug-cc-pV5Z basis set (2.000476 a.u.) with 105 basis functions. At this point, it is worth noticing that our results are of comparable accuracy to the best unextrapolated result reported by Matito et al. [66] for $\omega^2 = 0.25$, namely, 2.0002965 a.u., obtained using systematic sequences of Gaussian primitives with even-tempered exponents. Finally, the use of the aug-cc-pV6Z basis set, which contains 182 basis functions, leads only to a minor improvement in the energy, 2.000196 a.u. Moreover, this basis set shows large linear dependencies, and in fact, the total number of molecular orbitals in the variational space is reduced to 139 upon elimination of linear dependencies. This fact has led us not to consider this basis set any further in this current work. Besides, two more basis sets have been tested, which will be referred as aug-cc-pV5Z* and aug-cc-pV6Z*. This basis set are created by removing the basis functions with angular momentum greater or equal to four. The reduction in size of the basis set is substantial, from 105 to 75 for aug-cc-pV5Z, and from 182 to 95 for aug-cc-pV6Z. Moreover, the latter basis set upon removal of *g* and *h* basis functions does not show linear dependencies. The reduction of basis set size has only minor effects in the energy. In the case of aug-cc-pV5Z basis set, the energy increases only from 2.000476 to 2.000685 a.u., whereas for aug-cc-pV6Z, from 2.000196 to 2.000426 a.u. Considering the performance of our optimized ETBS-6S basis set, it gives a value for the singlet of 2.000396 a.u., that is, the second lowest energy value and only improved by the considerably higher aug-cc-pV6Z basis set.

The triplet-singlet gap (Δ_{T-S}), in eV, for two-electron systems can be found in Table 1. Irrespective of the basis set employed in the calculation, the lowest energy orbital is of *s*-type, followed by a shell of *p* orbitals [14]. We will call these orbitals the 1*s* and 1*p* orbitals. Hence, the singlet state is formed by the double occupation of the 1*s* orbital and the triplet state corresponds to the promotion of one of the 1*s* electrons to one 1*p* orbital plus a one-spin flip. The triplet-singlet gap is large. At the Full-CI/aug-cc-pV6Z level of theory, the gap is 9.86 and 9.78 eV for Full-CI/ETBS-6S, a very similar value to our reference value of 9.79 eV, which fully justifies the use of our ETBS-6S basis set as a good compromise between accuracy and computational cost. On the other hand, the better performance of the ETBS-6S basis set over the Dunning ones is more evident when more electrons are considered (see below), and therefore, we will discuss in the manuscript the results for the ETBS-6S basis set, in comparison with some values for the aug-cc-pV6Z* basis set. The results for the rest of the Dunning's basis sets can be found in Table S1.

Since the use of Full-CI is prohibitive as the number of electrons increases, we have analyzed the performance of CASSCF and MRMP2 methods, using the ETBS-6S basis sets. In Table 2, we report the energies obtained at the CASSCF and MRMP2 levels of theory using different active spaces. The results can also be visualized in Figure 1, where we have analyzed the convergence of CASSCF (dashed line) and MRMP2 (continuum line) as we consider more orbitals (N_{orb} in the active window). We consider from a minimal window of 2 orbitals up to 13 orbitals, which correspond to the 1*s*, 1*p*, 1*d*, 2*s*, and 2*p* shells. The convergence in Δ_{T-S} is obtained quite fast, specially for MRMP2 method, with an excellent agreement with Full-CI results.

3.2 | Four-electron systems

The results for the four-electron systems can be found in Tables 3 and S1, and in Figure 1. In this case, the use of Full-CI was computationally prohibitive. On the other hand, multideterminantal wave functions are mandatory due to substantial near-degeneracy effects. Consequently, we have decided to use multiconfigurational wave functions of the CASSCF type. We have investigated active spaces that span from 4 to 13 orbitals, corresponding to the 1*s*, 1*p*, 1*d*, 2*s*, and 2*p* shells. We have included the four electrons in this active orbital space and consider all possible

TABLE 1 HF and full-CI energies of the singlet and triplet spin states for the two-electron Hooke atom ($\omega^2 = 0.25$; $\lambda_{ee} = 0.0$)

Basis	Size	Contraction	Singlet HF (a.u.)	Singlet FCI (a.u.)	Triplet FCI (a.u.)	Δ_{T-S} (eV)
aug-cc-pVDZ	9	(5s2p/3s2p)	2.087904	2.055213	2.386080	9.00
aug-cc-pVTZ	25	(7s3p2d/4s3p2d)	2.038634	2.004107	2.373537	10.05
aug-cc-pVQZ	55	(8s4p3d2f/5s4p3d2f)	2.038443	2.001484	2.383204	10.39
aug-cc-pV5Z[a]	75	(9s5p4d3f/6s5p4d3f)	2.038408	2.000685	2.373767	10.15
aug-cc-pV6Z[a]	95	(11s6p5d4f/7s6p5d4f)	2.038423	2.000426	2.362738	9.86
aug-cc-pV5Z	105	(9s5p4d3f2g/6s5p4d3f2g)	2.038400	2.000476	2.373701	10.16
aug-cc-pV6Z	182	(11s6p5d4f3g2h/7s6p5d4f3g2h)	2.038404	2.000196	2.362579	9.86
ETBS-6S	80	(4s4p4d4f/4s4p4d4f)	2.038400	2.000396	2.359673	9.78

[a]Modified basis set removing basis functions with $l \geq 4$.

TABLE 2 HF, CAS(2, N_{orb}), and MRMP2(2, N_{orb}) energies with the ETBS-6S basis set, in atomic units, for the singlet and triplet spin states of the two-electron Hooke atom

		CAS(N_e, N_{orb})			MRMP2(N_e, N_{orb})		
Basis	N_{orb}	Singlet	Triplet	Δ_{T-S} (eV)	Singlet	Triplet	Δ_{T-S} (eV)
	2	2.026787	2.364478	9.19	2.006140	2.360420	9.64
	3	2.016225	2.364478	9.48	2.003759	2.360428	9.70
	4	2.006551	2.364478	9.74	2.001197	2.360601	9.78
	5	2.003410	2.362773	9.78	2.000701	2.360358	9.79
	6	2.003056	2.361106	9.74	2.000670	2.359828	9.77
	7	2.002705	2.361106	9.75	2.000637	2.359819	9.77
	8	2.002358	2.361106	9.76	2.000601	2.359820	9.77
	9	2.002019	2.361106	9.77	2.000559	2.359821	9.78
	10	2.001681	2.361106	9.78	2.000516	2.359828	9.78
	11	2.001630	2.359907	9.75	2.000513	2.359694	9.77
	12	2.001280	2.359859	9.76	2.000481	2.359687	9.77
	13	2.001082	2.359821	9.76	2.000461	2.359688	9.77
	FCI	2.000396	2.359673	9.78			
aug-cc-pV6Z*	13	2.001203	2.362886	9.84	2.000483	2.362749	9.86
aug-cc-pV6Z*	FCI	2.000426	2.362738	9.86			
Reference [14]		2.000000	2.359657	9.79			

Note: The RHF energy for the singlet state is 2.038400 and 2.038423 a.u. for the ETBS-6S and aug-cc-pV6Z* basis sets, respectively.
*stands for: "Modified basis set removing basis functions with l ≥ 4".

excitations within the window that are compatible with the desired spin state (singlet or triplet). The starting orbitals for the CASSCF calculations correspond to the HF orbitals of the singlet state. The biggest calculation using 4 electrons and 13 orbitals for the CAS window leads to 2366 configuration state functions (CSFs) for the singlet state, and 3003 CSFs for the triplet state. We have also considered second-order perturbation corrections based on these CASSCF wavefunctions (MRMP2, hereafter).

The electronic structure of the singlet state presents double occupation of the *1s* orbital and one of the *1p* orbitals. The triplet state corresponds mainly to a configuration in which the *1s* orbital is doubly occupied and two *1p* orbitals have one electron each. Due to the degeneracy of the *1p* shell, the resultant singlet and triplet CASSCF wavefunctions show large nondynamical correlation or near-degeneracy effects, and, therefore, the need to use multiple configurations in the wavefunction.

As one can see in Tables 3 and S1, the values of Δ_{T-S} are negative for all basis sets and methods considered, indicating that in the case of four electrons the confinement has led to a triplet-spin ground state. Notice from Figure 1 that the convergence of the results with the window size is quite fast. The values of the triplet-singlet gap at the CAS(4, 13) and MRMP2(4, 13) levels of theory with the aug-cc-pV6Z* basis set are −1.11 and −1.08 eV, respectively, in nice agreement with the reference value by Cioslowski et al. [21] of −1.00 eV. The use of the ETBS-6S basis sets slightly improves these results, giving values of −1.06 and −1.04 eV at the CAS(4, 13) and MRMP2(4, 13) levels of theory. However, we can see that the CAS(4, 13)/ETBS-6S energies are significantly closer to the reference values than the CAS(4, 13)/aug-cc-pV6Z* ones. For instance, the

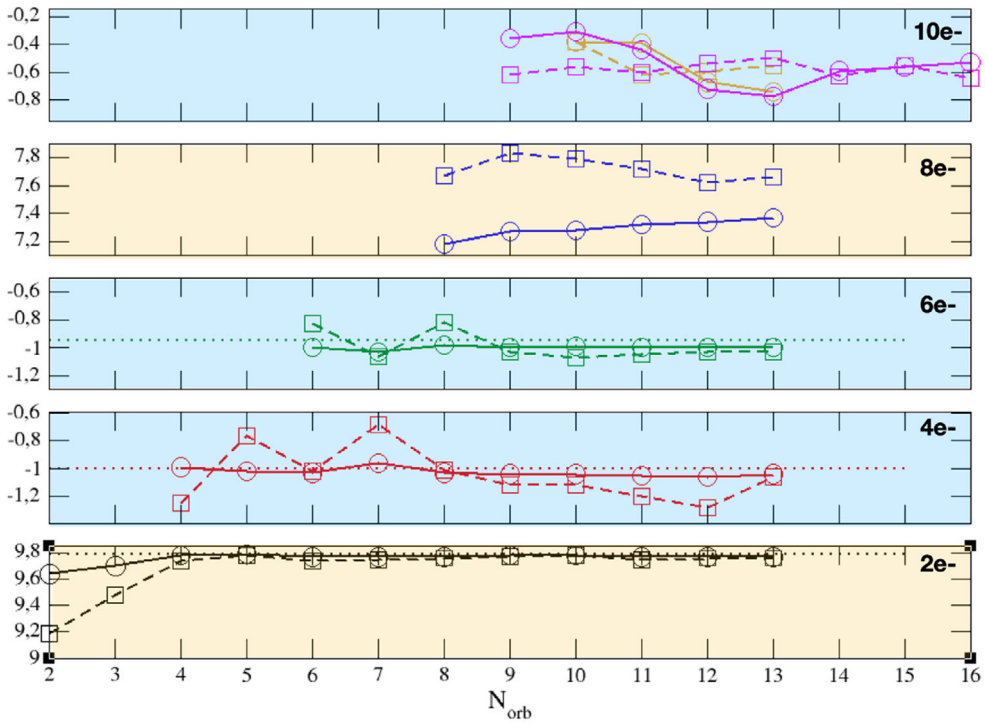

FIGURE 1 Triplet-singlet energy gap, in eV, calculated at the CAS(N_e, N_{orb}) (dashed line) and MRMP2(N_e, N_{orb}) (continuous line) levels of theory with the ETBS-6S basis set, as a function of the number of orbitals N_{orb} included in the active space. All cases correspond to a CASSCF wavefunction in which all electrons are included in the active space, except for the curves in magenta for the 10-electron system, that correspond to wavefunctions in which the 1s orbital occupation is set to 2, and therefore, the active space is composed of eight electrons and $N_{orb} - 2$ orbitals

TABLE 3 HF, CAS(4, N_{orb}), and MRMP2(4, N_{orb}) energies with ETBS-6S basis set, in atomic units, for the singlet and triplet spin states of the four-electron Hooke atom

		CAS(4, N_{orb})			MRMP2(4, N_{orb})		
Basis	N_{orb}	**Singlet**	**Triplet**	Δ_{T-S} **(eV)**	**Singlet**	**Triplet**	Δ_{T-S} **(eV)**
	4	6.466497	6.420487	−1.25	6.393971	6.357443	−0.99
	5	6.436891	6.409056	−0.76	6.395878	6.358352	−1.02
	6	6.432908	6.395502	−1.02	6.395253	6.357424	−1.03
	7	6.412845	6.387924	−0.68	6.391439	6.356035	−0.96
	8	6.416955	6.379714	−1.01	6.392298	6.354322	−1.03
	9	6.412845	6.371627	−1.12	6.391439	6.353215	−1.04
	10	6.410052	6.368950	−1.12	6.391231	6.352928	−1.04
	11	6.409228	6.365185	−1.20	6.391078	6.352579	−1.05
	12	6.408315	6.361114	−1.28	6.390980	6.352180	−1.06
	13	6.398720	6.359758	−1.06	6.390085	6.352024	−1.04
aug-cc-pV6Z*	13	6.412708	6.371770	−1.11	6.403958	6.364288	−1.08
Reference [21]		6.385543	6.348830	−1.00			

Note: The RHF energy or the singlet state is 6.505162 and 6.517905 a.u. for the EBTS-6S and aug-cc-pV6Z* basis sets, respectively.
*stands for: "Modified basis set removing basis functions with l ≥ 4".

energy value for the singlet and triplet states are 6.398720 and 6.359758 a.u., respectively, in good agreement with the values of Cioslowski et al. [21] 6.385543 and 6.348830 a.u., respectively. The introduction of second-order perturbation corrections, albeit non-variational, further improves this agreement, giving energies, 6.390085 and 6.352024, that are even closer to the ones by Cioslowski et al. [21] An advantage of the MRMP2 energies (see Figure 1) is that they are less dependent on the active space of the CASSCF wavefunction and, thus, we can use a smaller

TABLE 4 HF, CAS(6, N_{orb}), and MRMP2(6, N_{orb}) energies with ETBS-6S basis set, in atomic units, for the singlet and triplet spin states of the four-electron Hooke atom

		CAS(6, N_{orb})			MRMP2(6, N_{orb})		
Basis	N_{orb}	**Singlet**	**Triplet**	Δ_{T-S} **(eV)**	**Singlet**	**Triplet**	Δ_{T-S} **(eV)**
	6	12.177056	12.154962	−0.60	12.091183	12.055694	−0.97
	7	12.171843	12.132887	−1.06	12.089361	12.051390	−1.03
	8	12.147118	12.117039	−0.82	12.086838	12.050945	−0.98
	9	12.137934	12.099985	−1.03	12.085660	12.048808	−1.00
	10	12.132401	12.094292	−1.04	12.084591	12.047936	−1.00
	11	12.126035	12.087898	−1.04	12.083819	12.047183	−1.00
	12	12.120721	12.082893	−1.03	12.083437	12.046636	−1.00
	13	12.114932	12.077925	−1.01	12.082804	12.046141	−1.00
aug-cc-pV6Z*	13	12.149632	12.110496	−1.06	12.120797	12.082391	−1.05
Reference [48]		12.066294	12.031275	−0.95			

Note: The RHF energy or the singlet state is 12.253446 and 12.287010 a.u. for the EBTS-6S and aug-cc-pV6Z* basis sets, respectively.
*stands for: "Modified basis set removing basis functions with l ≥ 4".

active space without sacrificing the accuracy. The singlet-triplet gap obtained with MRMP2(4, 13) is −1.04 eV, also in very good agreement with the one by Cioslowski et al.[21]

3.3 | Six-electron systems

The results for the six-electron systems can be found in Tables 4 and S1, and in Figure 1. As in the previous case, we use CASSCF type wavefunctions, with different active spaces that go from a minimal 6 orbital window up to 13 orbitals (1*s*, 1*p*, 1*d*, 2*s*, and 2*p*), and include all six electrons. Our largest CAS window involves 26 026 CSFs for the singlet state, and 39 039 for the triplet.

The inclusion of two further electrons in the 1*p*-shell yields a very similar triplet-singlet gap and trends close to the ones observed for four-electron systems. Again, we obtain negative values for Δ_{T-S}, indicating that the ground state is a triplet. For instance, the value of Δ_{T-S} is −1.03 and −1.0 eV at the CAS(6, 13)/ETBS-6S and MRMP2(6, 13)/ETBS-6S levels of theory. A glance at Figure 1 clearly demonstrates that the results are very well converged with respect to the window size, specially for the MRMP2 level of theory. The values for the aug-cc-pV6Z* basis set are very similar, namely, −1.06 and −1.05 eV. Our results for the singlet-triplet gap agree satisfactorily with the reference calculations for the six-electron Hookean atom [48], which yield a value of −0.95 eV with an energy of 12.066294 a.u. for the singlet and 12.031275 a.u. for the triplet. In the case of the six-electron system, ETBS-6S absolute energies again give a significant improvement over the aug-cc-pV6Z* ones. However, now the difference between our CASSCF/ETBS-6S and the reference energies of Strasburger [48] increases with respect to the four-electron case. For instance, CAS(6, 13)/ETBS-6S energies are 12.115772 and 12.077925 a.u. for singlet and triplet states, respectively, whereas the reference energies are 12.066294 and 12.031275 a.u. However, the introduction of perturbation corrections lowers the energies to 12.082805 and 12.046142 a.u at the MRMP2(6, 13)/ETBS-6S level of theory, yielding a triplet-singlet gap only differing by 0.05 eV with respect to the −0.95 eV gap obtained from the data of Strasburger [48]. In summary, although the quality of our absolute energies of each of the states decreases with the increasing number of electrons, the estimation of the triplet-singlet gap remains correct.

3.4 | Eight-electron systems

Tables 5 and S1, and Figure 1 summarize the results for eight-electron systems, using CASSCF wavefunctions with an active space composed of 8–13 orbitals (1*s*, 1*p*, 1*d*, 2*s*, and 2*p* orbitals) and eight electrons. In the case of our largest window, the CASSCF(8, 13) wavefunction yields 143 143 CSFs for the singlet state, and 234 234 CSFs for the triplet. The corresponding second-order perturbative corrections can also be found in Table 5.

In the case of the singlet state, the eight-electron system corresponds to an electronic configuration in which the 1*s* and 1*p* shells are filled. In the case of the triplet state, based on the analysis of the occupancies of natural orbitals, an electronic configuration of $1s^2 1p^5 1d^1$-type is observed with ETBS-6S and aug-cc-pV6Z* basis sets, however, lower quality basis sets can yield an electronic configuration of $1s^2 1p^5 2s^1$-type (see Table S1). In other words, the gap between the 2*s* and 1*d* orbitals is sufficiently small so as to be sensible to the type of basis set. However,

TABLE 5 HF, CAS(8, N_{orb}), and MRMP2(8, N_{orb}) energies with ETBS-6S basis set, in atomic units, for the singlet and triplet spin states of the four-electron Hooke atom

		CAS(8, N_{orb})			MRMP2(8, N_{orb})		
Basis	N_{orb}	**Singlet**	**Triplet**	Δ_{T-S} (eV)	**Singlet**	**Triplet**	Δ_{T-S} (eV)
	8	19.113340	19.395160	7.67	19.008248	19.272166	7.18
	9	19.083985	19.371303	7.82	19.003255	19.270391	7.27
	10	19.075987	19.362461	7.79	19.000736	19.268463	7.28
	11	19.069697	19.353362	7.72	19.000079	19.269118	7.32
	12	19.063989	19.343947	7.62	18.999332	19.269118	7.34
	13	19.053174	19.334793	7.66	18.997973	19.268892	7.37
aug-cc-pV6Z*	13	19.110238	19.437774	8.91	19.065563	19.386165	8.72
Reference [19]		19.038	19.430	10.6			

Note: The RHF energy or the singlet state is 19.190980 and 19.247016 a.u. for the EBTS-6S and aug-cc-pV6Z* basis sets, respectively.
*stands for: "Modified basis set removing basis functions with l ≥ 4".

our best basis set, according to the criteria of the lowest triplet energy, favors the $1s^2 1p^5 1d^1$ configuration and, therefore, we conclude that our orbital ordering is 1*s* < 1*p* < 1*d* < 2*s* < 2*p*. This behavior reminds the situation that one encounters in transition metal atoms regarding the 3*d*/4*s* orbital ordering.

Irrespective of the type of configuration adopted, it is clear that the ground state of the eight-electron system is a singlet state, and presents a substantial gap with the triplet state, 7.66 eV at the CAS(8, 13)/ETBS-6S level of theory and 7.37 eV at the MRMP2(8, 13)/ETBS-6S level of theory. The latter results are reasonable well converged with respect to the CAS window size (see Figure 1). The triplet-singlet gap is significantly smaller than the one found for the two-electron case, namely, 9.78 eV. This result suggests a decrease of the inter-shell gap as we move along this series: 1*s* > 1*p* > 1*d*. However, our results differ significantly from the results of Varga et al. [19], which reported a gap of 10.6 eV. A closer inspection to the absolute energies can clarify this difference. Our singlet and triplet CAS(8, 13)/ETBS-6S energies are 19.05314 and 19.334793 a.u, respectively. When perturbation corrections are included the values are 18.997973 and 19.268892 a.u. The most accurate eight-electron Hooke atom results found in the literature up to date correspond to the ones of Varga et al. [19] which are 19.038 and 19.430 a.u., leading to a gap of 10.6 eV, much higher than our triplet-singlet gap. However, notice that our variational value for the triplet state is lower than the results obtained by Varga et al. [19] for their lowest triplet state, which suggests that we have been able to obtain a more accurate result for this state. In addition, since our results for four- and six-electron systems show a better agreement with the reference data, we believe that they are of higher accuracy than the ones of Varga et al. [19] for the eight-electron system. It is worth mentioning that some discrepancy with the three-electron case published by Varga [19] has been reported in the literature [20].

3.5 | Ten-electron systems

To the best of our knowledge, for the 10-electron system, there are not previous calculations in the literature. Tables 6 and S1, and Figure 1, summarize the results for the 10-electron systems. We used CASSCF wavefunctions with an active space composed of 10–13 orbitals (1*s*, 1*p*, 1*d*, 2*s*, and 2*p* orbitals) and 10 electrons. For the CASSCF(10, 13) wavefunction, this yields 429 429 CSFs for the singlet state, and 736 164 CSFs for the triplet. Regarding the dominant electronic configuration, this is of $1s^2 1p^6 1d^2$ type for both singlet and triplet state. It is worth noticing that there is an important discrepancy among the various aug-cc type basis sets on the nature of the Aufbau principle for the 10-electron system, with the aug-cc-pV6Z* basis set favoring the filling of 1*d* orbitals (as for ETBS-6S), while the rest of the basis-sets favor the filling of a 2*s* orbital (see Table S1). This has importance consequences in the relative energies of the singlet and triplet states, giving a singlet ground electronic state in the case that the filling of a 2*s* orbital is favored, whereas a triplet ground state is obtained in the case that the filling of the 1*d* shell is prioritized.

This highlights the importance of optimizing an appropriate basis set, which is adapted to the external potential of the system, like the ETBS-6S one. A remarkable aspect is that the Aufbau structure 1*s* > 1*p* > 1*d* remains throughout the whole 2-, 4-, 6-, 8-, and 10-electron series with the ETBS-6S basis set, since in all cases we obtain higher fractional occupation numbers for 1*d* orbitals than for the 2*s* one.

Using the ETBS-6S basis set, and irrespective of the method used, the triplet state is lower in energy than the singlet state, with a gap smaller than the one found for the four- and six-electron cases. Hence, when passing from 8- to 10-electron, the system changes the spin state of the ground state of the system. Our best estimate is −0.55 eV at CAS(10, 13)/ETBS-6S level of theory and −0.74 eV at MRMP2(10, 13)/ETBS-6S.

The convergence of the triplet-singlet gap with respect to N_{orb} is less satisfactory than for the cases of a lower number of electrons (see Figure 1). We also noticed that the natural orbital occupation associated to the 1*s* orbital in the 10-electron case is always higher than 1.98.

TABLE 6 HF, CAS(10, N_{orb}), and MRMP2(10, N_{orb}) energies with ETBS-6S basis set, in atomic units, for the singlet and triplet spin states of the four-electron Hooke atom

		CAS(10, N_{orb})			MRMP2(10, N_{orb})		
Basis	N_{orb}	Singlet	Triplet	Δ_{T-S} (eV)	Singlet	Triplet	Δ_{T-S} (eV)
	10	27.828015	27.807466	−0.56	27.675164	27.665330	−0.27
	11	27.813009	27.790373	−0.62	27.678880	27.664692	−0.39
	12	27.795515	27.773761	−0.59	27.688082	27.663346	−0.67
	13	27.777241	27.757081	−0.55	27.689185	27.661990	−0.74
aug-cc-pV6Z*	13	28.020989	28.007019	−0.38	27.951539	27.937691	−0.38

Note: The RHF energy or the singlet state is 27.932821 and 28.174226 a.for the EBTS-6S and aug-cc-pV6Z* basis sets, respectively.
*stands for: "Modified basis set removing basis functions with l ≥ 4".

Therefore, we decided to remove this orbital and the two associated electrons form the CAS window, which allowed us to expand further the window size to include more virtual orbitals at a reasonable computational cost. When the occupation of the 1*s* orbital is set to 2.0 (magenta curve in Figure 1), we obtain almost identical values of the triplet-singlet gap to the case in which the 1*s* orbital and its electrons participate in the definition of the CAS window (orange curve in Figure 1). One can see in the figure that now we get quite well converged results finding a triplet-singlet gap of −0.64 eV at CASSCF(8, 15)/ETBS-6S level of theory and −0.53 eV at MRMP2(8, 15)/ETBS-6S level of theory, further confrming the triplet nature of the ground state of the 10-electron Hooke atom, and the smaller triplet-singlet gap with respect to the cases of four and six electrons.

3.6 | Screened Hooke atom

Due to the fact that the results for $N_e = 2$-, 4-, 6-, and 8-electron systems were quite converged for a window of 10 orbitals, we have considered the CASSCF(N_e, 10)/ETBS-6S and MRMP2(N_e, 10)/ETBS-6S methods to analyze the effect that the screening of the electron–electron interaction has on the triplet-singlet gap. In the case of the 10-electron system, we used the CAS(10, 10)/ETBS-6S and MRMP2(10, 10)/ETBS-6S methods, but we also performed CAS(8, 14)/ETBS-6S and MRMP2(8, 14)/ETBS-6S calculations, which are more converged results with respect to the window size, as demonstrated in the previous section. We have increased progressively the amount of screened electron–electron interactions by considering values of λ_{ee} of 0.2, 0.4, 0.6, 0.8, and 1.0; the results are summarized in Table 7 and Figure 2.

The nature of the spin of the ground state is not altered upon inclusion of screening effects (see Figure 2A, top figure), namely 2- and 8-electron cases show singlet ground states, whereas 4-, 6-, and 10-electron cases have triplet ground states. Nevertheless, the triplet-singlet gap is sensitive to the degree of electron–electron screening, specially in the case of two and eight electrons. This is due to the fact that, based on the *Aufbau* principle, these systems form closed-shell structures for singlet spin states; hence, every two electrons share the same spatial orbital and interact strongly through two-body interacting. In these two cases, the introduction of screening effects produces a very substantial and gradual stabilization of the singlet state over the triple one (see Figure 2B). Therefore, the reduction of the electronic repulsion leads to a more favorable spin pairing in these two systems. Thus, in the case of the two-electron Hooke atom, there is an increase in Δ_{T-S} from 9.78 to 11.51 eV when passing from full Coulombic to Yukawa $\lambda = 1.0$ screened electron–electron potential at MRMP2(2, 10)/ETBS-6S level of theory. This increase in Δ_{T-S} is even higher for the eight-electron case, from 7.28 to 10.48 eV. Notice that in these two cases the triplet is formed by promoting one electron to the next shell with higher angular momentum, and thus, our results suggest that the introduction of screening effects among the electrons results in a stabilization of the lower angular momentum shells, leading to larger gaps between the shells, and therefore, more pronounced triplet-singlet gaps.

On the other hand, the 4-, 6-, and 10-electron cases are less affected by the screening of the electron–electron interactions (Figure 2A). These three cases show triplet ground states and the introduction of screening has again a stabilizing effect of the singlet state over the triplet one (see Figure 2B) but to a much lesser extent than in the case of two- and eight-electron systems. Thus, in the case of four electrons, Δ_{T-S} changes from −1.04 to −0.78 eV, in the case of six electrons goes from −0.99 to −0.77 eV, and in the case of ten electrons from −0.56 to −0.34 eV. Notice however, that even though in terms of absolute numbers this is a small effect, the screening of electron–electron interactions has been able to reduce almost to half the *S*/*T* gap in the case of 10-electron system. In general, we may conclude that there is a clear stabilization of the singlet over the triplet state upon screening effects, but this stabilization is not as large as to revert the nature of the spin of the ground state.

3.7 | Decomposing the energy into different contributions

To get further insights of the different contributions into the above mentioned trends, in Table 8, we can find the decomposition of the total energy into kinetic, confinement and electron–electron repulsion terms for the 2-, 4-, 6-, 8-, and 10-electron Hooke atoms and the corresponding screened ($\lambda_{ee} = 1.0$) Hooke atoms, using the CAS(N_e, 10)/ETBS-6S energies.

TABLE 7 HF, CAS(N_e, 10), and MRMP2(N_e, 10) energies, in atomic units, for the singlet and triplet spin states of the s-Hooke model at different values of the λ screening parameter

	HF	CAS(N_e, 10)			MRMP2(N_e, 10)		
λ	Singlet	Singlet	Triplet	Δ_{T-S} (eV)	Singlet	Triplet	Δ_{T-S} (eV)
Two-electron							
0.0	2.038400	2.001681	2.361106	9.78	2.000516	2.359828	9.78
0.2	1.879433	1.845903	2.212892	9.99	1.844644	2.211584	9.98
0.4	1.777898	1.750206	2.131426	10.37	1.748859	2.130299	10.38
0.6	1.710108	1.688101	2.084166	10.78	1.686715	2.083500	10.80
0.8	1.663091	1.645841	2.055639	11.15	1.644470	2.055161	11.17
1.0	1.629427	1.615941	2.037805	11.48	1.614631	2.037480	11.51
Four-electron							
0.0	6.505162	6.410052	6.368950	−1.12	6.391231	6.352928	−1.04
0.2	4.447821	5.522013	5.481478	−1.10	5.502540	5.464743	−1.03
0.4	5.098802	5.027175	4.988257	−1.06	5.008695	4.972340	−0.99
0.6	4.786937	4.729994	4.692890	−1.01	4.712556	4.678623	−0.92
0.8	4.584830	4.539335	4.505120	−0.93	4.524068	4.492776	−0.85
1.0	4.447821	4.411219	4.380074	−0.85	4.398160	4.369611	−0.78
Six-electron							
0.0	12.253446	12.133679	12.094292	−1.07	12.084454	12.047936	−0.99
0.2	10.066994	9.960398	9.921242	−1.07	9.909188	9.873006	−0.98
0.4	8.877716	8.792459	8.754633	−1.03	8.745296	8.710196	−0.96
0.6	8.171402	8.104086	8.069290	−0.95	8.064118	8.030753	−0.91
0.8	7.723094	7.671069	7.638238	−0.89	7.636670	7.605815	−0.84
1.0	7.424057	7.382940	7.353003	−0.81	7.354441	7.326141	−0.77
Eight-electron							
0.0	19.190980	19.075987	19.362461	7.79	19.000736	19.268463	7.28
0.2	15.182763	15.084400	15.384014	8.15	15.005631	15.289623	7.73
0.4	13.068595	12.994991	13.317898	8.79	12.922972	13.235696	8.51
0.6	11.834935	11.781507	12.128228	9.43	11.719577	12.060148	9.27
0.8	11.060156	11.021423	11.389781	10.02	10.969653	11.334431	9.93
1.0	10.547028	10.518701	10.905855	10.53	10.475994	10.861138	10.48
10-electron							
0.0	27.932821	27.828015	27.807466	−0.56	27.675164	27.665330	−0.27
0.2	21.621750	21.528857	21.511339	−0.48	21.375745	21.363283	−0.34
0.4	18.408818	18.334295	18.317410	−0.46	18.203431	18.190047	−0.36
0.6	16.573893	16.515099	16.499172	−0.43	16.408780	16.395457	−0.36
0.8	15.437499	15.390866	15.376062	−0.40	15.305881	15.293178	−0.35
1.0	14.692340	14.654914	14.641306	−0.37	14.587232	14.575380	−0.32

First, we analyze the different contributions to the triplet-singlet gap for the unscreened Hooke atom. We find two clear different patterns for the singlet (two- and eight-electron systems) and triplet ground states (4-, 6-, and 10-electron cases). In all cases, the electron–electron repulsion term is always negative, favoring the triplet state over the singlet one. However, while for 4-, 6-, and 10-electron systems, the $\Delta^{V_{ee}}_{T-S}$ is the leading term that governs the overall triplet-singlet gap, for two and eight electrons, this term is of lower magnitude than the kinetic Δ^{K}_{T-S} and the confinement terms $\Delta^{V_{conf}}_{T-S}$. Thus, the promotion of one electron to the next shell, as it happens in the triplet state of two- and eight-electron systems, results in a very high increase of the kinetic and confinement energies, that cannot be overcome by the lower electron–electron repulsion of the triplet state. However, the formation of the triplet states in 4-, 6-, and 10-electron systems corresponds to intra-shell promotions, with very small differences in the kinetic energy between singlet and triplet states and with a confinement contribution that favors the triplet over the singlet, although its magnitude is smaller than the energy gain obtained by decreasing the electron–electron repulsion.

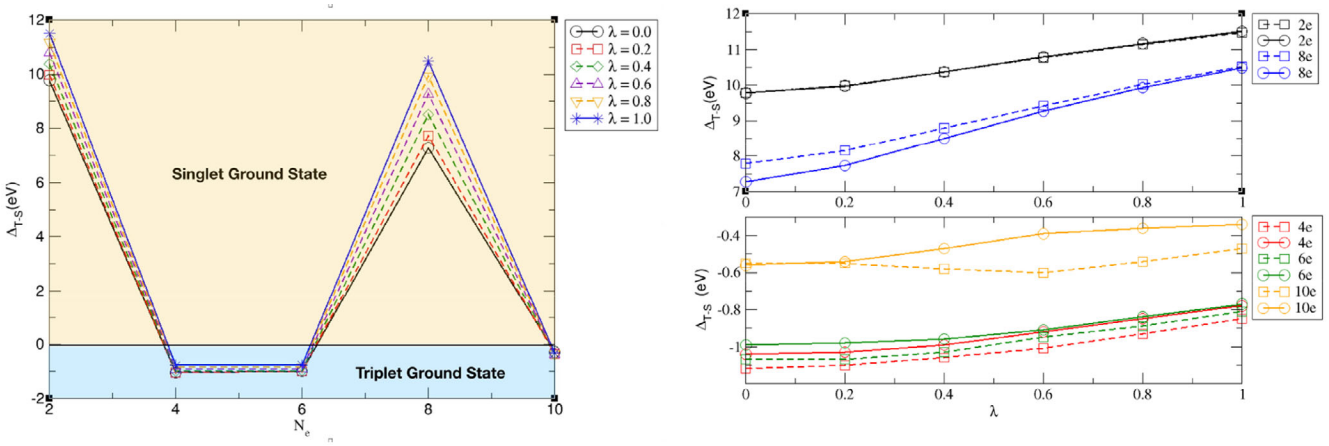

FIGURE 2 (A) Left figure: Triplet-singlet energy gap, in eV, calculated at the MRMP2(N_e, 10) level of theory (2-, 4-, 6-, and 8-electron systems) and MRMP2(8, 14) (10-electron system), as a function of the number of electrons and for different values of λ. (B) Right Figure: Triplet-singlet energy gap, in eV, calculated at CAS(N_e, 10) (dashed line) and MRMP2(N_e, 10) (continuous line) levels of theory for 2, 4, 6, and 8 electrons, and CAS(8, 14) (dashed line) and MRMP2(8, 14) (continuous line) levels of theory for the 10-electron system, as a function of the degree of screening (λ). All calculations were done with the ETBS-6S basis set

We analyze now the influence of screening on the different components of the energy. We have selected a $\lambda_{ee} = 1.0$ to perform this analysis. As one can see in Table 8, this value of λ_{ee} implies a very effective screening of the electron–electron interactions with a reduction between 78.1% and 89.6% of the electron–electron repulsion energy. As expected, this is the main energy component affected by the introduction of the screening. Nevertheless, the confinement and kinetic contributions are also substantially affected, with an increase in the kinetic energy and a lowering of the confinement energy, as the number of electrons increases. Thus, the increase in kinetic energy goes from a 5.8% in two-electron systems to 34% in 10-electron systems, whereas the reduction in confinement energy goes from 6% to 8% in singlet and triplet two-electron cases to 28% when 10 electrons are considered. These trends can be explained in terms of a more compact electronic density upon reduction of the electron–electron repulsion, which augments the kinetic energy and reduces the confinement energy.

The influence of screening in the different contributions to Δ_{T-S} can also be found in Table 8. Again, we see different trends for two- and eight-electron cases, and for 4-, 6-, and 10-electron cases. For two- and eight-electron Hooke atoms, there is an important reduction in the electron–electron repulsion contribution to the triplet-singlet gap, which favors the singlet state by roughly 1 eV. In addition, due to the fact that there is an increase in the energy gap between shells upon screening, the confinement and kinetic energy contributions also augment and favor the singlet state. Therefore, in the two- and eight-electron systems, the three contributions to Δ_{T-S} increase, and substantially favors the singlet state over the triplet one. In the case of four- and six-electron systems, the reduction in the electron–electron repulsion is very similar in both the triplet and singlets states and, therefore, its contribution to the changes in Δ_{T-S} is minimal. In these two cases, the kinetic Δ^K_{T-S} term is the main contributor to the slight changes in triplet-singlet gap upon screening. Finally, in 10-electron systems, both kinetic and electron–electron repulsion contribute equally. Nevertheless, the differences in these terms when introducing electron–electron screening are very small compared to the two- and eight-electron systems, and highlights the difference between inter- and intra-shell promotion when building the triplet state.

3.8 | Coulomb holes

Finally, in order to gain a deeper insight of the electron correlation effects, we have also calculated the Coulomb holes for the Coulombic and Yukawa confined ($\lambda_{ee} = 1.0$) systems. The Coulomb holes, $h(u)$, are defined as the difference in the intracule density, $I(u)$, of a correlated wavefunction, CASSCF(N, 13) in our case, and an uncorrelated one, RHF or ROHF for singlet and triplet states, respectively.

$$h(u) = I^{\mathrm{CASSCF}}(u) - I^{\mathrm{RHF/ROHF}}(u) \tag{5}$$

with $u = |r_{12}|$. The radial intracule density provides a distribution of the electron–electron distances and it is defined as,

$$I(u) = \iint n_2(r_1, r_2)\delta(u - r_{12})dr_1 dr_2 \tag{6}$$

TABLE 8 Decomposition of the total energy (a.u.) of the singlet and triplet states into different contributions, kinetic energy, confinement energy (that is the one corresponding to the monoelectronic harmonium confinement operator), and electron–electron repulsion energy

		Singlet energy components (a.u.)				Triplet energy components (a.u.)				Triplet single gap (eV)			
N_e	Model	Kin. E.	V_{conf}	V_{ee}	Total E.	Kin. E.	V_{conf}	V_{ee}	Total E.	Δ^{K}_{T-S}	$\Delta^{V_{ee}}_{T-S}$	$\Delta^{V_{conf}}_{T-S}$	Δ_{T-S}
2	Hooke	0.664231	0.888647	0.448803	2.001681	0.920322	1.093808	0.346977	2.361106	6.97	5.58	−2.77	9.78
	s-Hooke	0.702495	0.815055	0.098391	1.615941	0.974102	1.027525	0.036178	2.037805	7.39	5.78	−1.69	11.48
	Δ_{s-u}	0.038264	−0.073592	−0.350412	−0.385740	0.053780	−0.066283	−0.310799	−0.323301	0.42	0.20	1.08	1.70
	$\%\Delta_{s-u}$	5.8	−8.3	−78.1	−19.3	5.8	−6.06	−89.6	−13.7				
4	Hooke	1.575643	2.661960	2.172449	6.410052	1.575087	2.648067	2.145797	6.368950	−0.02	−0.38	−0.73	−1.12
	s-Hooke	1.802488	2.247689	0.361041	4.411219	1.810012	2.234690	0.335372	4.380074	0.20	−0.35	−0.70	−0.85
	Δ_{s-u}	0.226845	−0.414271	−1.811408	−1.998833	0.234925	−0.413377	−1.810425	−1.988876	0.22	0.03	0.03	0.27
	$\%\Delta_{s-u}$	14.4	−15.6	−83.4	−31.2	14.9	−15.61	−84.4	−31.2				
6	Hooke	2.298682	4.810967	5.024030	12.133679	2.296848	4.797225	5.000219	12.094292	−0.05	−0.37	−0.65	−1.07
	s-Hooke	2.815149	3.794034	0.773756	7.382940	2.821571	3.781367	0.750065	7.353003	0.17	−0.30	−0.64	−0.81
	Δ_{s-u}	0.516467	−1.016933	−4.250274	−4.750739	0.524723	−1.015858	−4.250154	−4.741289	0.22	0.03	0.01	0.26
	$\%\Delta_{s-u}$	22.5	−21.1	−84.6	−39.2	22.8	−21.18	−85.0	−39.2				
8	Hooke	2.889288	7.320715	8.865985	19.075987	3.129535	7.489993	8.742933	19.362461	6.54	4.61	−3.35	7.79
	s-Hooke	3.755694	5.445591	1.317417	10.518701	4.034318	5.638694	1.232843	10.905855	7.58	5.25	−2.30	10.53
	Δ_{s-u}	0.866406	−1.875124	−7.548568	−8.557286	0.904783	−1.851299	−7.510090	−8.456606	1.04	0.64	1.05	2.74
	$\%\Delta_{s-u}$	30.0	−25.6	−85.1	−44.9	28.9	−24.72	−85.9	−43.7				
10	Hooke	3.857152	10.517423	13.453440	27.828015	3.857015	10.511402	13.439049	27.807466	0.00	−0.16	−0.39	−0.56
	s-Hooke	5.168257	7.609567	1.877090	14.654914	5.171068	7.603958	1.866280	14.641306	0.08	−0.15	−0.29	−0.37
	Δ_{s-u}	1.311105	−2.907856	−11.576350	−13.173101	1.314053	−2.907444	−11.572769	−13.166160	0.08	0.01	0.10	0.19
	$\%\Delta_{s-u}$	34.0	−27.6	−86.0	−47.3	34.1	−27.66	−86.1	−47.3				

Note: Decomposition of the triplet-singlet gap Δ_{T-S} into kinetic confinement and electron–electron repulsion terms. Two cases are considered: (i) Hooke atom with standard Coulombic interactions between electrons and (ii) s-Hooke in which the electron–electron interactions are screened by the Yukawa potential with $\lambda_{ee} = 1.0$. Δ_{s-u} corresponds to the differences between the screened and unscreened calculation.

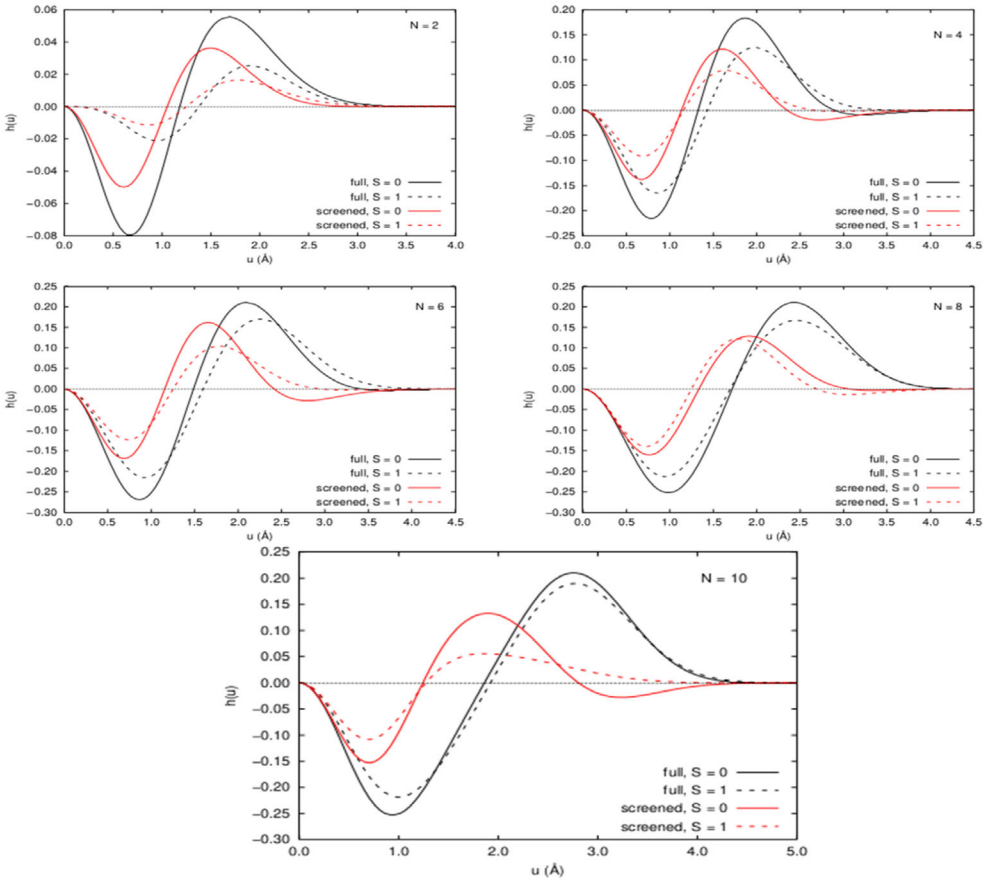

FIGURE 3 Coulomb holes calculated at the CASSCF(N, 13)/ETBS-6S level of theory for both full (solid lines) and $\lambda_{ee} = 1.0$ screened-Coulombic (dashed lines) Hooke systems with different number of electrons ($N = 2$, 4, 6, 8, and 10) and for singlet (black lines) and triplet states (red lines)

where n_2 ($\mathbf{r}_1$, $\mathbf{r}_2$) is the pair density and r_{12} is the module of the intracular coordinate, namely, the interelectronic distance. Thus, the intracule density gives the probability of finding any two electrons at a certain distance u. The Coulomb hole is a measure of how electron correlation affects the probability of finding two electrons at a given distance. As this function only depends on the interelectronic distance, it provides a simple visualization of the distribution of electron–electron separations; by monitoring the changes in this distribution. We may gain further knowledge of the behavior of electron correlation in these systems and how this is affected by the number of electrons, spin state and screening of electron–electron interaction.

Results are displayed in Figure 3. A common pattern is observed irrespective of the number of electrons: (*i*) the Coulomb hole is more pronounced for singlet than for triplet states in both full Coulombic and screened systems and (*ii*) the introduction of screening effects results in a significant reduction of the corresponding Coulomb holes. As expected, in general, the main effect of introducing electron correlation effects is an increase in the interelectronic distance, namely, the Coulomb holes show a depletion at short distances and a concomitant rise at larger distances. However, an interesting feature arises for screened systems in the case of singlet states with 4, 6, and 10 electrons: there is a depletion of the Coulomb hole at large distances. This feature is also observed to a lower extent for the eight-electron screened system with a triplet spin multiplicity. Therefore, in these cases, electrons are correlated in such way that they come closer compared to the Coulomb potential due to the attractive interaction at large distances. This can be explained by the tendency mentioned in the previous section of a more compact electronic cloud in screened systems, which leads to a reduction of the confinement energy. Our results point to a relationship of the intrashell electron–electron correlation (as it occurs for singlet 4-, 6-, and 10-electron and triplet 8-electron systems), with the promotion of a more compact electronic cloud.

4 | CONCLUDING REMARKS

In the present paper, we have presented a thorough study of 2-, 4-, 6-, 8-, and 10-electron systems confined in a spherical quantum dot in their singlet and triplet spin states, with the aim of determining the triplet-singlet gap for Hooke-type systems. The effect of screening the electron–electron interaction has also been taken into account effectively by the introduction of a Yukawa type potential.

Our results show an interesting pattern in the triplet-singlet gap as the number of electrons increases. Thus, singlet state is the ground state for 2 and 8, whereas the triplet state is the ground spin state in four-and six-electron systems. The situation for 10-electron system is again a triplet ground state, but with a gap smaller than the one found for four and six electrons. Our results can be readily rationalized in terms of the following orbital ordering $1s < 1p < 1d$, with a decrease in the successive energy gaps.

We have also observed that the screening of electron–electron interaction has a sizable effect, not only on the absolute energies for each state, but also on the triplet-singlet gap. The triplet-singlet gap for the two electron and eight electron cases is specially sensible to the screening effect, favoring the singlet state over the triplet. This can be related to an increase of the corresponding gap between shells upon screening. However, the influence of screening in the triplet-singlet gap for 4-, 6-, and 10-electron cases was much more reduced, favoring again the singlet state but, in no case, this screening produced a switch between spin states.

AUTHOR CONTRIBUTIONS

Xabier Telleria-Allika: Data curation; formal analysis. **Jesus Ugalde:** Conceptualization. **Eduard Matito:** Conceptualization; writing – original draft. **Eloy Ramos-Cordoba:** Conceptualization; data curation. **Mauricio Rodríguez-Mayorga:** Data curation; formal analysis. **Xabier Lopez**: Data production, analysis, writing, programming,

ACKNOWLEDGMENTS

This research was funded by Eusko Jaurlaritza (the Basque Government), through Consolidated Group Project No. IT1584-22, PIBA19-0004, and 2019-CIEN-000092-01, and the Spanish MINECO/FEDER Projects No. PGC2018-097529-B-100, PGC2018-098212-B-C21, EUIN2017-88605, and EUR2019-103825. Eloy Ramos-Cordoba acknowledges funding from the Juan de la Cierva program IJCI-2017-34658. Technical and human support provided by IZO-SGI, SGIker (UPV/EHU, MICINN, GV/EJ, ERDF, and ESF) is gratefully acknowledged.

DATA AVAILABILITY STATEMENT

The data that support the findings of this study are available from the corresponding author upon reasonable request.

ORCID

Jesus M. Ugalde https://orcid.org/0000-0001-8980-9751
Eduard Matito https://orcid.org/0000-0001-6895-4562
Eloy Ramos-Cordoba https://orcid.org/0000-0002-6558-7821
Mauricio Rodríguez-Mayorga https://orcid.org/0000-0003-0869-9787
Xabier Lopez https://orcid.org/0000-0002-2711-3588

REFERENCES

[1] D. Gammon, *Nature* **2000**, *405*, 899.
[2] L. V. Dias da Silva, C. H. Lewenkopf, N. Studart, *Phys. Rev. B* **2004**, *69*, 075311.
[3] E. Barnes, J. P. Kestner, N. T. T. Nguyen, S. S. Das, *Phys. Rev. B* **2011** Dec, *84*, 235309.
[4] C. Ellenberger, T. Ihn, C. Yannouleas, U. Landman, K. Ensslin, D. Driscoll, A. C. Gossard, *Phys. Rev. Lett.* **2006**, *96*, 126806.
[5] H. Yakobi, E. Eliav, U. Kaidor, *J. Chem. Phys.* **2011**, *134*, 054503.
[6] B. DeMarco, D. S. Jin, *Science* **1999**, *285*, 1703.
[7] A. G. Truscott, K. E. Strecker, W. I. McAlexander, G. B. Partridge, R. G. Hulet, *Science* **2001**, *291*, 2570.
[8] B. Pingault, D. D. Jarausch, C. Hepp, L. Klintberg, J. N. Becker, M. Markham, C. Becher, M. Atatüre, *Nat. Commun.* **2017**, *8*, 15579.
[9] Y. Zhou, A. Rasmita, Q. K. Li, Xiong, I. Aharonovich, W.-B. Gao, *Nat. Commun.* **2017**, *8*, 14451.
[10] S. M. Reimann, M. Manninen, *Rev. Mod. Phys.* **2002** Nov, *74*, 1283.
[11] L. W. Wang, A. Zunger, *Phys. Rev. B* **1999** Jun, *59*, 15806.
[12] G. Bester, *J. Phys. Condens. Matter* **2008**, *21*(2), 023202.
[13] E. V. Ludeña, X. Lopez, J. M. Ugalde, *J. Chem. Phys.* **2005**, *123*, 024102.
[14] M. Taut, *Phys. Rev. A* **1993**, *48*, 3561.
[15] V. Sahni, *Quantal Density Functional Theory II*, Springer, Berlin **2014**.
[16] P. Gori-Giorgi, A. Savin, *Int. J. Quantum Chem.* **2009**, *109*(11), 2410.
[17] W. Zhu, S. B. Trickey, *J. Chem. Phys.* **2006**, *125*(9), 094317.
[18] M. Pedersen Lohne, G. Hagen, M. Hjorth-Jensen, S. Kvaal, F. Pederiva, *Phys. Rev. B* **2011** Sep, *84*, 115302.
[19] K. Varga, P. Navratil, J. Usukura, Y. Suzuki, *Phys. Rev. B* **2001**, *63*(20), 205308.
[20] J. Cioslowski, K. Strasburger, E. Matito, *J. Chem. Phys.* **2012**, *136*(19), 194112.
[21] J. Cioslowski, K. Strasburger, E. Matito, *J. Chem. Phys.* **2014**, *141*(4), 044128.
[22] R. C. Ashoori, H. L. Stormer, J. S. Weiner, L. N. Pfeiffer, K. W. Baldwin, K. W. West, *Phys. Rev. Lett.* **1993**, *71*, 613.
[23] D. Pfannkuche, S. E. Ulloa, *Phys. Rev. Lett.* **1995**, *74*, 1194.
[24] P. S. Drouvelis, P. Schmelcher, F. K. Diakonos, *Phys. Rev. B* **2004**, *69*, 035333.
[25] P. A. Maksym, H. Imamura, G. P. Mallon, H. Aoki, *J. Phys. Condens. Matter* **2000** may, *12*(22), R299.

[26] D. Heitmann, V. Gudmundsson, M. Hochgräfe, R. Krahne, D. Pfannkuche, *Phys. E* **2002**, *14*, 37.
[27] J. Adamowski, A. Kwaśniowski, B. Szafran, *J. Phys. Condens. Matter* **2005**, *17*, 4489.
[28] E. Ramos-Cordoba, P. Salvador, E. Matito, *Phys. Chem. Chem. Phys.* **2016**, *18*, 24015.
[29] E. Ramos-Cordoba, E. Matito, *J. Chem. Theory Comput.* **2017**, *13*, 2705.
[30] M. Via-Nadal, M. Rodríguez-Mayorga, E. Ramos-Cordoba, E. Matito, *J. Phys. Chem. Lett.* **2019**, *10*(14), 4032.
[31] P. Hessler, J. Park, K. Burke, *Phys. Rev. Lett.* **1999**, *82*, 378.
[32] P. M. Laufer, J. B. Krieger, *Phys. Rev. A* **1986**, *33*(3), 1480.
[33] S. Kais, D. R. Hersbach, N. C. Handy, C. W. Murray, G. J. Laming, *J. Chem. Phys.* **1993**, *99*, 417.
[34] C. Filippi, C. J. Umrigar, M. Taut, *J. Chem. Phys.* **1994**, *100*, 1290.
[35] C. J. Huang, C. J. Umrigar, *Phys. Rev. A* **1997**, *56*, 290.
[36] M. Taut, A. Ernst, H. Eschrig, *J. Phys. B* **1998**, *31*, 2689.
[37] Z. Qian, V. Sahni, *Phys. Rev. A* **1998**, *57*, 2527.
[38] S. Ivanov, K. Burke, M. Levy, *J. Chem. Phys.* **1999**, *110*, 10262.
[39] E. V. Ludeña, V. Karasiev, A. Artemiev, D. Gómez, in *Functional N-representability in Density Matrix and Density Functional Theory: An illustration for Hooke's Atom* (Ed: J. Cioslowski), Kluwer Academic/Plenum Publishers, New York **2000**.
[40] J. Cioslowski, E. Matito, *J. Chem. Theory Comput.* **2011**, *7*, 915.
[41] J. Cioslowski, M. Piris, E. Matito, *J. Chem. Phys.* **2015**, *143*(21), 214101.
[42] M. Rodríguez-Mayorga, E. Ramos-Cordoba, F. Feixas, E. Matito, *Phys. Chem. Chem. Phys.* **2017**, *19*, 4522.
[43] M. Rodríguez-Mayorga, E. Ramos-Cordoba, M. Via-Nadal, M. Piris, E. Matito, *Phys. Chem. Chem. Phys.* **2017**, *19*, 24029.
[44] J. Cioslowski, K. Pernal, *J. Chem. Phys.* **2000**, *113*, 8434.
[45] J. Cioslowski, E. Matito, *J. Chem. Phys.* **2011**, *134*(11), 116101.
[46] C. Amovilli, N. H. March, *Phys. Rev. A* **2011**, *83*(4), 044502.
[47] J. Cioslowski, *J. Chem. Phys.* **2013**, *139*(22), 224108.
[48] K. Strasburger, *J. Chem. Phys.* **2016**, *144*(23), 234304.
[49] J. Cioslowski, K. Strasburger, *J. Chem. Phys.* **2017**, *146*(4), 044308.
[50] J. Cioslowski, K. Strasburger, *J. Chem. Phys.* **2018**, *148*(14), 144107.
[51] P. A. Maksym, T. Chakraborty, *Phys. Rev. B* **1992**, *45*, 1947.
[52] J. M. Kinaret, Y. Meir, N. S. Wingreen, P. A. Lee, X. G. Wen, *Phys. Rev. B* **1992**, *46*, 4681.
[53] P. Hawrylak, *Phys. Rev. Lett.* **1993**, *71*, 3347.
[54] D. Pfannkuche, V. Gudmundsson, P. A. Maksym, *Phys. Rev. B* **1993**, *47*, 2244.
[55] S. R. E. Yang, A. H. MacDonald, D. M. Johnson, *Phys. Rev. Lett.* **1993**, *71*, 3194.
[56] J. J. Palacios, L. Martin-Moreno, G. Chiappe, E. Louis, C. Tejedor, *Phys. Rev. B* **1994**, *50*, 5760.
[57] de C Chamon C, Wen XG., *Phys. Rev. B* **1994**, *49*, 8227.
[58] M. Fujito, A. Natori, H. Yasunaga, *Phys. Rev. B* **1996**, *53*, 9952.
[59] C. Yannouleas, U. Landmann, *Phys. Rev. Lett.* **1999**, *82*, 5325.
[60] T. M. Henderson, K. Runge, R. J. Bartlett, *Chem. Phys. Lett.* **2001**, *337*, 138.
[61] M. Macucci, K. Hess, G. J. Iafrate, *Phys. Rev. B* **1993**, *48*, 17354.
[62] M. Koskinen, M. Manninen, S. M. Raimann, *Phys. Rev. Lett.* **1997**, *79*, 1389.
[63] H. Hirose, N. S. Wingreen, *Phys. Rev. B* **1999**, *59*, 4604.
[64] M. Gattobigio, P. Capuzzi, M. Polini, R. Asgari, M. P. Tossi, *Phys. Rev. B* **2005**, *72*, 045306.
[65] A. V. Filinov, M. Bonitz, Y. E. Lozovik, *Phys. Rev. Lett.* **2001**, *86*, 3851.
[66] E. Matito, J. Cioslowski, S. F. Vyboishchikov, *Phys. Chem. Chem. Phys.* **2010**, *12*, 6712.
[67] E. Santos, *An. R. Soc. Esp. Fís. Quím.* **1968**, *64*, 117.
[68] N. R. Kestner, O. Sinanoglu, *Phys. Rev.* **1962**, *128*, 2687.
[69] M. W. Schmidt, K. K. Baldridge, J. A. Boatz, S. T. Elbert, M. S. Gordon, J. H. Jensen, S. Koseki, N. Matsunaga, K. A. Nguyen, S. Su, T. L. Windus, M. Dupuis, J. A. Montgomery, *J. Comput. Chem.* **1993**, *14*, 1347.
[70] M. S. Gordon, M. W. Schmidt, Advances in electronic structure theory: GAMESS a decade later. in *Theory and Applications of Computational Chemistry, The First Forty Years* (Eds: C. E. Dykstra, G. Frenking, K. S. Kim, G. E. Scuseria), Elsevier, Amsterdam **2005**.
[71] M. Rodríguez-Mayorga, E. Ramos-Cordoba, X. Lopez, M. Solà, J. M. Ugalde, E. Matito, *ChemistryOpen* **2019**, *8*(4), 411.

SUPPORTING INFORMATION

Additional supporting information can be found online in the Supporting Information section at the end of this article.

How to cite this article: X. Telleria-Allika, J. M. Ugalde, E. Matito, E. Ramos-Cordoba, M. Rodríguez-Mayorga, X. Lopez, *Int. J. Quantum Chem.* **2023**, *123*(3), e27019. https://doi.org/10.1002/qua.27019